Bioinspired supramolecular fibers drawn from a multi-phase self-assembled hydrogel

Yuchao Wu[a,b,c], **Darshil U. Shah**[a,d], **Chenyan Liu**[b,c], **Ziyi Yu**[c], **Ji Liu**[b,c], **Xiaohe Ren**[b,c], **Matthew J. Rowland**[b,c], **Chris Abell**[c], **Michael H. Ramage**[d], **and Oren A. Scherman**[*b,c]

[a]Contributed equally to the work; [b]Melville Laboratory for Polymer Synthesis; [c]Department of Chemistry, University of Cambridge, Cambridge, CB2 1EW, United Kingdom; [d]Department of Architecture, University of Cambridge, Cambridge, CB2 1PX, United Kingdom

This manuscript was compiled on May 18, 2017

Inspired by biological systems, we report a supramolecular polymer-colloidal hydrogel (SPCH) comprising 98 wt% water that can be readily drawn into uniform (*ca.* 6 μm thick) 'supramolecular fibers' at room temperature. Functionalized polymer-grafted silica nanoparticles, a semi-crystalline hydroxyethyl cellulose derivative and cucurbit[8]uril undergo aqueous self-assembly at multiple length scales to form the SPCH, facilitated by host-guest interactions at the molecular level and nano-fibril formation at colloidal length scale. The fibers exhibit a unique combination of stiffness and high damping capacity (60-70%), the latter exceeding that of even biological silks and cellulose-based viscose rayon. The remarkable damping performance of the hierarchically-structured fibers is proposed to arise from the complex combination and interactions of 'hard' and 'soft' phases within the SPCH and its constituents. SPCH represent a new class of hybrid supramolecular composites, opening a window into fiber technology through low-energy manufacturing.

Supramolecular fibers | Hydrogel | Self-assembly |

In nature, spiders spin silk fibers with superb properties at ambient temperatures and pressures(1, 2). We are yet to mimic such an elegant process. Conventionally, synthetic fibers are manufactured through a variety of spinning techniques, including wet, dry, gel and electro-spinning(3). Such approaches to generate fibers are limited by high energy input, laborious procedures and intensive use of organic solvents. Supramolecular pathways enable the formation of filamentous soft materials that are showing promise in biomedical applications(4–6), such as cell culture(7–9) and tissue engineering(10). However, such materials are constrained by the length scale (sub-micron level)(11–13), energy intake duing production(9) and complex design of assembly units(14).

Here, we report drawing supramolecular fibers of arbitrary length from a dynamic, supramolecular polymer-colloid hydrogel (**SPCH**) at room temperature (Movie S1). The components consist of methyl viologen (MV) functionalised polymer-grafted silica nanoparticles (NP)s (**P1**), a semi-crystalline polymer in the form of a hydroxyethyl cellulose derivative (**H1**) and cucurbit[8]uril (CB[8]) as illustrated in Fig. 1. The macrocycle CB[8] is capable of simultaneously encapsulating two guests within its cavity, forming a stable yet dynamic ternary complex, has been exploited as a supramolecular 'handcuff' to physical crosslink fuctional polymers (15–18). Introducing shape-persistent nano-particles into the supramolecular hydrogel system allows for modification of the local gel structures at the colloidal length scale, resulting in assemblies with unique emergent properties (19). The hierarchical nature of the **SPCH** is presented, where the hydrogel is composed of nanoscale fibrillar structures. The self-assembled **SPCH** composite exhibits great elasticity at a remarkably high water content (98%), demonstrating a novel low-energy manufacturing process for fibers from natural, sustainable precursor materials. We hypothesized that the reorganisation of internal structures and the presence of crystallinity in the **SPCH** enable the formation of the 'supramolecular fiber'. Moreover, a detailed investigation of the mechanical behavior of these supramolecular fibers indicates they exhibit a unique combination of ductility and stiffness. These fibers are also remarkably efficient at absorbing energy with a high damping capacity, comparable to viscose, and in some ways, resembling the biological protein-based spider silks.

Results

Self-assembly of SPCH. The fabrication of SPCH was accomplished by mixing an aqueous solution of **H1** (1 wt%) with an aqueous solution of **P1** (1 wt%), which was previously complexed with CB[8] in a 1:1 MV:CB[8] ratio (**P1**@CB[8]). **P1** is a functional polymer (M_n = 74 kDa, polydispersity indext Đ= 1.48) grafted onto silica NPs with a core size of 50 nm (Fig. 1b, see SI Appendix, Fig. S1-6 for synthesis). The linear polymers (**H1** in Fig. 1b) were prepared by functionalizing napthalene (Np) isocyanate onto hydroxyethylcellulose (HEC; M_n = 1.3 MDa)(20). The composite material exhibited elastic behavior with an increase in rigidity and a persistent shape. The hydrogel formation is clearly dependent on the presence

Significance Statement

Fiber materials have great impact on our daily lives with their use ranging from textiles to functional reinforcements in composites. While the manufacturing process of man-made fibers is potentially limited by extensive energy consumption, spiders can readily spin silk fibers at room temperature. Here, we report a new class of material that is based on a self-assembled hydrogel constructed with dynamic host-guest cross-links between functional polymers. Supramolecular fibers can be drawn from this hydrogel at room temperature. The supramolecular fiber exhibits better tensile and damping properties than conventional regenerated fibers such as viscose, artificial silks and hair. Our approach offers a sustainable alternative to current fiber manufacturing strategies.

Y.W. and D.S. contributed equally to this work. Y.W. designed and synthesised polymers, prepared figures, analysed data and wrote the paper; D.S. performed tensile test experiments, prepared figures, analysed data and wrote the paper; C.L. synthesised molecules; Z.Y. analysed data, prepared figures. X.R., J.L. and M.J.R. analysed data; C.A., M.H.R. and O.A.S. supervised the experimental design, analysed data and wrote the paper.

The authors declare no competing financial interests.

[a]Y.W. and D.S. contributed equally to this work.

[*]To whom correspondence should be addressed. E-mail: oas23cam.ac.uk

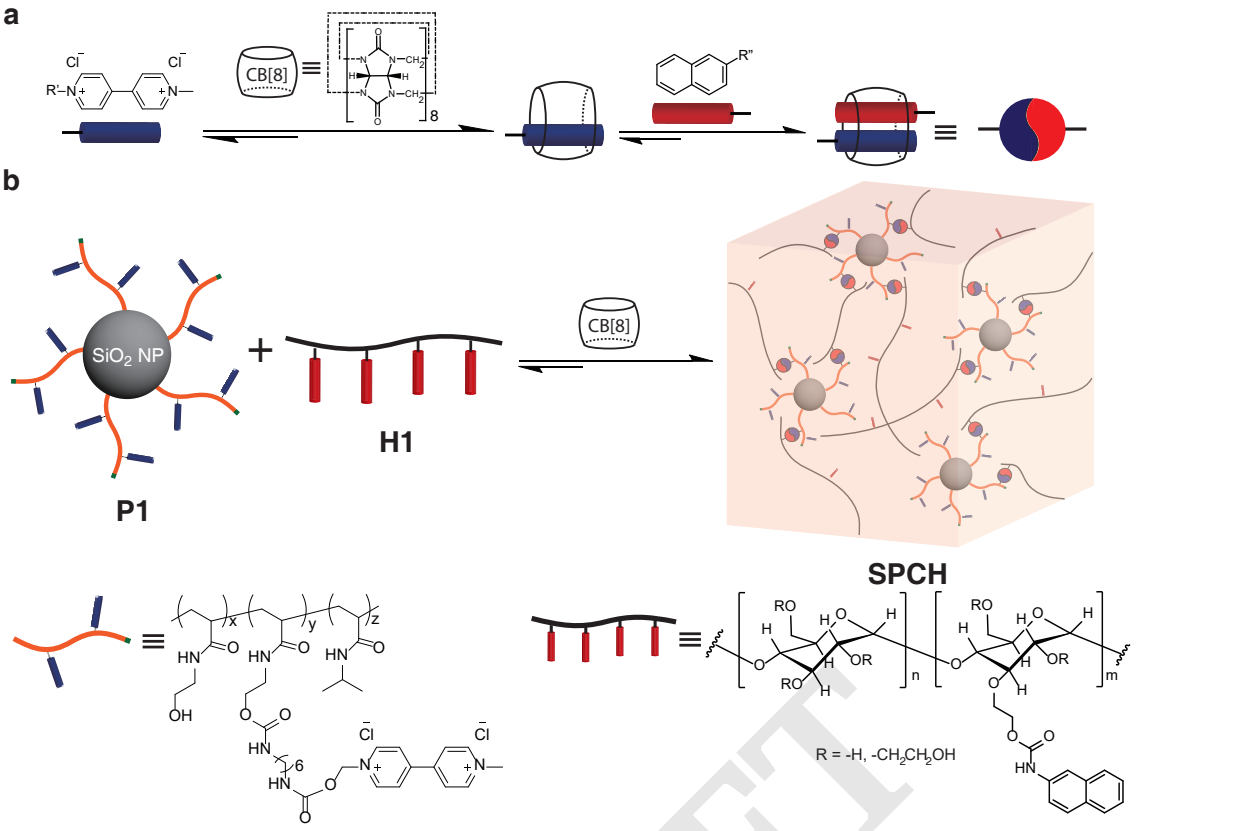

Fig. 1. Self-assembly of SPCH. a, Schematic of the two-step, three-component binding of cucurbit[8]uril in water. **b**, Schematic representation of a supramolecular hierarchical polymer-colloidal hydrogel prepared through addition of CB[8] to a mixture of polymer-grafted silica **P1** (functionalised with MV) and a linear HEC-NP **H1** in water.

of all three components of the ternary complex. In the absence of CB[8], or when CB[8] was replaced by CB[7], whose cavity is only large enough to encapsulate MV alone, mixtures of **H1** and **P1** behave like a runny liquid (Fig. 2a).

Mechanical properties of the hydrogels were investigated through rheological measurements. Strain dependent oscillatory rheology of a mixture of **H1** (1 wt%) with pre-complexed **P1**@CB[8] (1 wt%) displays a broad linear viscoelastic region with a gel-to-sol crossover point remarkably appearing only at 500% strain (Fig. 2b). The frequency-dependent rheology performed in the linear viscoelastic region is shown in Fig. 2c (blue circles), whereby storage moduli (G′) are dominant over loss moduli (G″) across the whole range of frequencies studied, which identifies gel-like behavior. In the absence of CB[8], no difference in the rheology was observed between an aqueous solution of **H1** (1 wt%) alone and a mixture of **H1** (1 wt%) with **P1** (1 wt%), indicating that entanglement arising from additional polymer chains **P1** does not lead to polymeric network formation (SI Appendix, Fig. S7–9). When **P1** was replaced with a larger silica NP size of 200 nm ($\mathbf{P}_{200}$) the assembled hydrogel became weaker as shown by the red squares in Fig. 2c, as the G″ becomes larger than G′ at low frequencies. This is possibly due to the reduction in the number of effective crosslinks in the hydrogel network (21). In addition, a rapid recovery rate of the material is observed in step-strain measurements depicted in Fig. 2d, where alternating strains of 1% and 1000% were applied to the material at 30 (s) intervals. Overall, the process was repeated over 5 cycles and the SPCH exhibited fast and complete recovery to its initial modulus, corresponding to the fast association kinetics of CB[8] ternary complexation (22, 23).

We observed that the hydrogels were substantially 'stretchy', revealing a highly ductile nature. Moreover, a 'filament' can be drawn from a reservoir of hydrogel (5 mg) at room temperature that remained stable to lengths > 250 mm (Fig. 3a) After the water in the hydrogel filament evaporates within 30 (s), a fine and flexible fiber remains with a cylindrical shape and consistent diameter as shown in the scanning electron microscopy (SEM) images in Fig. 3b and c. The fiber diameter was found to be independent of the draw length ($R^2 = 0.001$, n = 177; SI Appendix, Fig. S10), suggesting an increase in length during drawing was not at the expense of fiber diameter. Rather, fiber length increased through continuous drawing of material from the hydrogel reservoir and a simultaneous, rapid liquid-solid phase transition. We envisage that the fiber diameter is likely determined and therefore may be tuned by parameters such as gel viscosity, surface tension, environment (e.g. humidity), and using nozzles/orifices of specified dimensions. In addition, by slicing the cross-section of the 'supramolecular fiber' using focussed ion beam, we observed that the silica core NPs from **P1** were dispersively embedded in the fiber (Fig. 3d).

SEM was further used to investigate the internal structure of the **SPCH** in an effort to explain its unique ductility. Fig. 3e-g reveals the microstructure in the cross section of the cryo-dried and lyophilized hydrogel filament. As the magnification factor increases, we observed nanoscale fibrillar features that interweave and support the internal network of the hydrogel filament. When the diameter of the silica core increased,

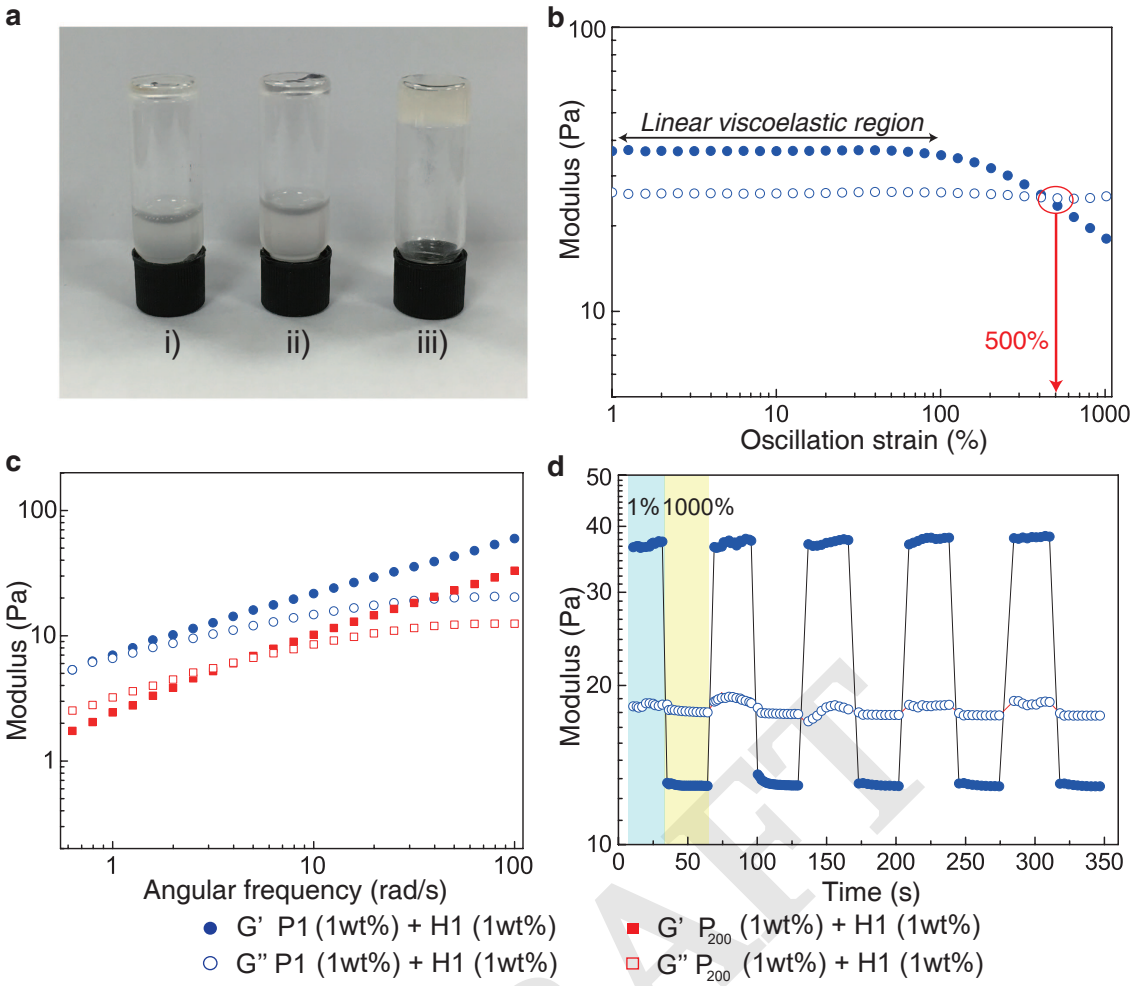

Fig. 2. Fabrication and rheological characterisation of the SPCH. a, Photograph of Inverted vial tests demonstrating the formation of the hydrogel from the mixture of **P1** (1 wt%), **H1** (1 wt%), and CB[8] (0.05 wt%) exclusively. Vial **i)**: **P1** and **H1**; Vial **ii)**: **P1**, **H1** and CB[7]; Vial **iii)**: **P1**, **H1** and CB[8]. **b**, Rheological strain oscillatory rheology of **P1** (1 wt%)@CB[8]/**H1** (1 wt%) from 0.1% to 1000% at 20 °C (ω = 10 rad/s). The materials expressed broad viscoelastic regimes and resisted yielding up to 100% strain, G′/G″ crossover point at 500%. **c**, Frequency dependent oscillatory rheology, demonstrating that hydrogels with polymer grafted on 50 nm silica NPs (**P1**) have stronger and more ordered networks than hydrogels with polymer grafted on 200 nm silica NPs ($\mathbf{P}_{200}$). **d**, Step-strain measurement with applied oscillatory strain alternated between 1 and 1000% for 30 s periods (ω = 10 rad/s, 20 °C). At high strain, G″ dominates. Upon alternating back to 1% strain, G′ recovers rapidly to its original viscoelastic property. This process was repeated across five high strain periods demonstrating good recyclability.

hydrogels assembled between $\mathbf{P}_{200}$@CB[8] and **H1** exhibited nanosheet-like internal structures (SI Appendix, Fig. S11) compared to the nanofibril features mentioned above, which resulted in unstable filaments (that break upon dehydration). This also correlates with the frequency sweep in the early rheology study (Fig. 2c, red squares). When **P1** was replaced with a linear polymer, poly(NIPAm-*co*-HEAm-MV) (**LP**), the hydrogel did not show such ductility, nor did it yield fibers (Movie S2). No nano-fibrillar microstructures were observed in the hydrogels (SI Appendix, Fig. S12) or for any previously reported CB[8]-based hydrogels. More importantly, the semi-crystalline **H1** (SI Appendix, Fig. S13) allows further enhancement of the elasticity, where the crystalline domain of the polymer chains could reconfigure themselves. To verify this as a generic theory, we prepared a hydrogel by replacing **H1** with Np functionalized polyvinyl alcohol (PVA) that is a typical semi-crystalline polymer. The resulting materials show similar transformations into fibers (SI Appendix, Fig. S14). In contrast, when amorphous functional polymers (poly(AM-co-HEAm-Np)) were assembled with **P1**@CB[8], no fiber formation was observed (SI Appendix, Fig. S15). Overall, **H1**, with crystalline domains at the molecular level, was assembled with **P1** through dynamic host-guest interactions *via* CB[8], forming the nanoscale fibrils, which extend, realign and repack at the colloidal length scale (Fig. 3h and i). The resulting 'hydrogel filament' (drawn from the **SPCH**) exhibits hierarchical structures across multiple length scales that distribute the applied stress effectively. Finally, the large aspect ratio of the filament induces fast evaporation of water, yielding a ductile supramolecular fiber.

Characterisation of the supramolecular fiber. Stress-strain profiles (Fig. 4a) display an initial linear region up to a yield point in the range of 1–3% applied strain (The tensile-testing method of fibers is described in the SI Appendix). The elastic modulus determined in this region was 6.0 ± 2.9 GPa. Most polymeric materials have stiffness in the range of 1 MPa to *ca.* 10 GPa. Our supramolecular fiber consists of multiple phases, some of which are soft (amorphous) at room temperature,

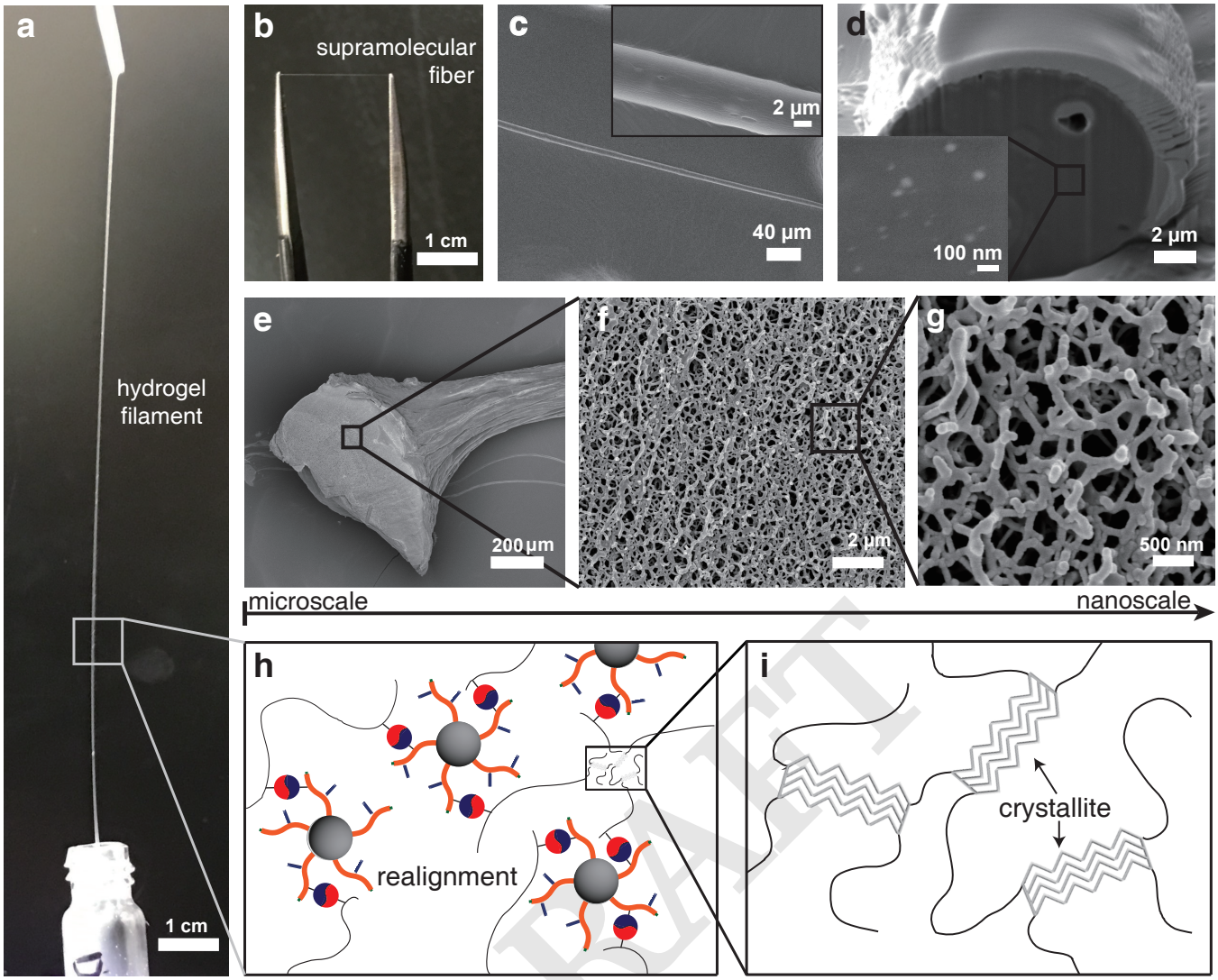

Fig. 3. Investigating the structure of SPCH. a, Photograph of the hydrogel filament drawn from the **SPCH** reservoir. **b**, Photograph of the supramolecular fiber after the hydrogel filament undergoes fast dehydration. **c**, Scanning electron microscopy image of the supramolecular fiber. **d**, Focussed ion beam scanning electron microscopy image of the cross-section area in the supramolecular fiber, the light-colored particles in the inset depict the silica NPs with size around 50 nm dispersed inside the polymer matrix. **e-g**, Cryogenic scanning electron microscopy images of the internal structure of **SPCH** demonstrate its hierarchical nature with nanoscale fibrils feature. **h,i**, Proposed molecular organization within the hydrogel filament, with **H1** and **P1** physically crosslinked by CB[8], and the **H1** polymer having crystalline domains.

and some of which are crystalline. The crystalline phases provide intermolecular interactions which are stable and do not exhibit viscosity at room temperature, thereby dominating the mechanical response and the resulting high stiffness. Failure strength and strain of the fiber were determined to be 193 ± 54 MPa and 18.1 ± 5.7%, respectively. This unique combination of tensile properties exceeds that of conventional regenerated textile fibers such as cellulose-based viscose, and protein-based artificial silks as well as animal and human hair(24) (SI Appendix, Fig. S17). Finally, the toughness, or total energy required to break the fiber, was calculated to be 22.8 ± 10.3 $MJ{\cdot}m^{-3}$, higher than several natural fibers, such as flax and jute (25). The coefficient of variation in properties ranged between 30 to 50%, which is a spread commonly observed in natural fibers including biological silk(26) and flax (27). Factors influencing variability include processing conditions (drawing speed), environmental conditions (during processing and testing) as well as the composition of the material (26, 28).

In an effort to assess reversibility and damping behavior of the supramolecular fiber, material response to cyclic loads was investigated. Fibers with low damping capacity (high resilience), like E-glass, elastin, polypropylene and vulcanised rubber are efficient at recovering most of the deformation energy they absorb, typically exhibiting little to no hysteresis; while fibers with high damping capacity (low resilience), such as viscose, cotton and silks are efficient at absorbing or dissipating most of the energy (Fig. 5). We subjected the fiber to a single load-unload-reload cycle (see Fig. 4b). It is evident that the supramolecular fiber has a high damping capacity of 64.2 ± 2.2% (n = 7), which is even higher than biological silks and comparable to viscose (Fig. 5). Furthermore, we find that the coefficient of variation in the damping capacity of our supramolecular fiber was significantly lower at only 3%, in comparison to that of all other mechanical properties (ranging between 30 to 50%). Thus, damping capacity in our case is

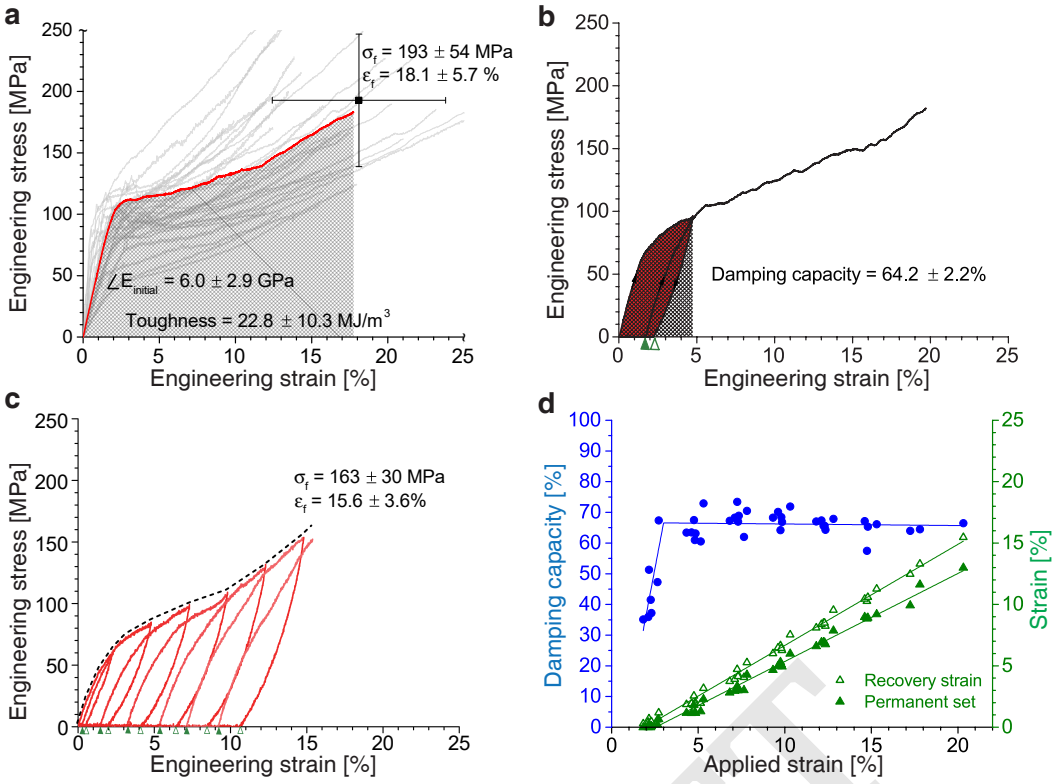

Fig. 4. Mechanical properties of supramolecular fibers subjected to static and cyclic tensile loads. a, Illustration of the fiber stress-strain response at a quasi-static loading rate: grey curves indicate variability in the dataset (n = 50), with a representative data curve shown in red; the data point (solid square) indicates the mean failure strength and strain, with error bars denoting 1 std. dev. **b**, Representative stress-strain curve (n = 7) of a fiber subjected to a single loading-unloading-reloading cycle (indicated by arrowheads) at 5% strain. The recovery strain (upon unloading) and the permanent set (before reloading) are indicated by hollow and solid triangles, respectively, on the x-axis. The damping capacity was determined from the ratio of the damping energy (shaded area; area between the loading and unloading curve) to the stored energy (hatched area; area below the loading curve). **c**, Representative stress-strain curve (n = 7) of a fiber subjected to progressive loading cycles at 2.5% strain intervals up to failure. The damping energy, indicated by the areas between the paired loading-unloading curves, increases with every loading cycle. **d**, The evolution of damping capacity, recovery strain and permanent set with applied strain. Linear fits to the data points are shown.

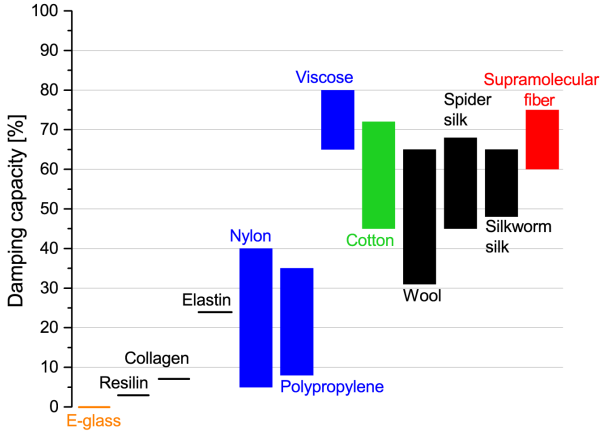

Fig. 5. Comparison of the mechanical properties of our supramolecular fiber (red) with other typical technical fibers. The damping capacity of the supramolecular fiber exceeds that of biological silks and is comparable to viscose, making it a good candidate for energy-absorption applications.

more directly related to the molecular structure of the fiber.

From further tests, we observed that damping energy as well as damping capacity reduced with respected cycles of loading-unloading: from 67.2 ± 5.3% in the first cycle to 31.2 ± 2.8% by the fifth cycle, with the major drop (of 60%) occurring between the first and second cycle (SI Appendix, Fig. S18). Essentially, by subjecting the supramolecular fiber to multiple cycles at the same applied strain it was transformed from being effective at energy dissipation to a material efficient at energy recovery and storage. Interestingly, this behavior has also been observed for spider silks whose damping capacity drops from around 68% in the first cycle to as low as 37% in subsequent cycles (29). When the supramolecular fiber was subjected to progressive loading-unloading cycles until failure, the damping energy was observed to increase with every cycle (Fig. 4c). Notably, while the damping capacity increased from 30 to 65% in the range of 2-3% applied strain (*i.e.* after the first cycle close to the yield point), it was remarkably stable at 66% for all other cycles of applied strain ranging between 3-20% (n = 7, Fig. 4d). The existence of damping capacity below the yield strain is likely to be because the supramolecular fibers are 'visco-elastic' (rather than 'purely elastic') below the yield point and 'visco-elasto-plastic' above the yield point. Again, such a profile has also been observed for spider silks, whose damping capacity is low (at 5 to 30%) in the first cycle at 5% applied strain, but increases to 30 to 70% in subsequent cycles of increasingly applied strain(30). The recovery strain and permanent set (permanent deformation) were also found to increase linearly with the applied strain (applied deformation) in every cycle up to failure (Fig. 4d).

We envision that the remarkable damping performance of

the supramolecular fiber arises from energy dissipative mechanisms provided by a complex structure of 'hard' (crystalline) and 'soft' (amorphous) phases at the molecular scale (*vis.* semi-crystalline **H1** polymer, Fig. 3i), like in spider silks(29, 31). While the soft phase is always active, the hard phase is strain-activated, and undergoes a partly-reversible transformation to the soft phase *via* a process of strain-induced hydrogen bond breakage when stretched to its limit, which is accompanied by the unravelling, aligning and slipping of molecular chains. The energy stored during loading in the previous process is (partly) released during unloading, by the reformation of hydrogen bonds and reverse-transition of soft phases to hard phases, as well as de-alignment or coiling of molecular chains. Consequently, the fiber finds itself in a new molecular conformation at a non-zero recovery strain (Fig. 4b)(29, 31). In the case of our supramolecular fiber, 'hard' and 'soft' phases exist beyond the molecular scale of the semi-crystalline **H1** polymer, at the intermolecular scale (where CB[8] provides dynamic cross-links between **P1** and **H1**), as well as at the colloidal scale (silica NPs in the **SPCH**, Fig. 3h).

Conclusion

We have shown a novel means of assembling hierarchical supramolecular polymer-colloidal hydrogels (**SPCH**) based on CB[8] host-guest chemistry. By introducing functional polymer grafted silica NPs, we successfully modified the internal structure of the gel at the nanoscale and benefit from the semi-crystalline nature of **H1**, which allow for significant enhancement of the elasticity of the material. We have reported for the first time a 'supramolecular fiber' drawn from an extremely high water-content **SPCH** at room temperature. The synthetic biocompatible fiber exhibits a unique combination of strength and high damping capacity that can be readily manipulated through a detailed understanding of the hierarchical assembled structure and the underlying CB[8] host-guest chemistry. We envision that by altering the chemistry and processing methods of **SPCH**, a family of supramolecular fibers with a whole range of tuneable properties can be produced at low temperature taking us a considerable step closer to sustainable fiber technology.

ACKNOWLEDGMENTS. This work was supported by the Engineering Physical Sciences Research Council (EPSRC) EP/K503496/1 and a Translational Grant EP/H046593/1 as well as a Leverhulme Trust Programme Grant (Natural Materials Innovation); Mr Y. Wu was funded EPSRC EP/L504920/1. The authors would like to acknowledge Dr J. Skepper and Dr J.J. Rickard for their detailed and helpful discussion on this manuscript.

1. Anna Rising and Jan Johansson. Toward spinning artificial spider silk. *Nat. Chem. Biol.*, 11 (5):309–15, 2015. ISSN 1552-4469. . URL http://www.ncbi.nlm.nih.gov/pubmed/25885958.
2. F Vollrath and D P Knight. Liquid crystalline spinning of spider silk. *Nature*, 410(6828):541–8, 2001. ISSN 0028-0836. . URL http://dx.doi.org/10.1038/35069000.
3. Andreas Greiner and Joachim H. Wendorff. Electrospinning: A fascinating method for the preparation of ultrathin fibers. *Angew. Chem. Int. Ed.*, 46(30):5670–5703, 2007. ISSN 14337851. .
4. G M Whitesides, J P Mathias, and C T Seto. Molecular self-assembly and nanochemistry: a chemical strategy for the synthesis of nanostructures. *Science (New York, N.Y.)*, 254(5036): 1312–9, 1991. ISSN 0036-8075. . URL http://www.ncbi.nlm.nih.gov/pubmed/1962191.
5. M. J. Webber, E. A. Appel, E. W. Meijer, and R. Langer. Supramolecular biomaterials. *Nature Materials*, 15:13–26, 2016.
6. T. Aida, E. W. Meijer, and S. I. Stupp. Functional supramolecular polymers. *Science*, 335: 813–817, 2012.
7. R.M. Capito, H.S. Azevedo, Y.S. Velichko, A. Mata, and S.I. Stupp. Self-assembly of large and small molecules into hierarchically ordered sacs and membranes. *Science*, 319:1812–1816, 2008.
8. Rebecca Nelson, Michael R Sawaya, Melinda Balbirnie, Anders Ø Madsen, Christian Riekel, Robert Grothe, and David Eisenberg. Structure of the cross-β spine of amyloid-like fibrils. *Nat. Cell Biol.*, 435(7043):773–778, 2005. ISSN 1476-4687. . URL http://www.nature.com/doifinder/10.1038/nature03680.
9. S. Zhang, M. A. Greenfield, A. Mata, Palmer L. C., R. Bitton, J. R. Mantei, C. Aparicio, M. O. d. l. Cruz, and S. I. Stupp. A self-assembly pathway to aligned monodomain gels. *Nature Materials*, 9:594–601, 2010.
10. P.Y.W. Dankers, M.C. Harmsen, M. J. A. V. Brouwer, L. A. abd Luyn, and E. W. Meijer. A modular and supramolecular approach to bioactive scaffolds for tissue engineering. *Nature Materials*, 4:568–574, 2005.
11. Anna Merzlyak, Shyam Indrakanti, and Seung Wuk Lee. Genetically engineered nanofiber-like viruses for tissue regenerating materials. *Nano Lett.*, 9(2):846–852, 2009. ISSN 15306984. .
12. Meital Reches and Ehud Gazit. Casting Metal Nanowires Within Discrete Self-Assembled Peptide Nanotubes. *Science*, 300(5619):625–627, 2003. ISSN 00368075. .
13. Jeffrey D. Hartgerink, Elia Beniash, and Samuel I. Stupp. Self-assembly and mineralization of peptide-amphiphile nanofibers. *Science*, 294(5547):1684–1688, 2001. ISSN 0036-8075. . URL http://science.sciencemag.org/content/294/5547/1684.
14. Takashi Kato, Norihiro Mizoshita, and Kenji Kishimoto. Functional liquid-crystalline assemblies: Self-organized soft materials. *Angew. Chem. Int. Ed.*, 45(1):38–68, 2005. ISSN 14337851. .
15. E. A. Appel, X. J. Loh, S. T. Jones, F. Biedermann, C. A. Dreiss, and O. A. Scherman. Ultrahigh-water-content supramolecular hydrogels exhibiting multistimuli responsiveness. *J. Am. Chem. Soc.*, 134:11767–11773, 2012.
16. Ji Liu, Yang Lan, Ziyi Yu, Cindy S.Y. Tan, Richard M. Parker, Chris Abell, and Oren A. Scherman. Cucurbit[n]uril-based microcapsules self-assembled within microfluidic droplets: A versatile approach for supramolecular architectures and materials. *Acc. Chem. Res.*, 50(2): 208–217, jan 2017. .
17. Ji Liu, Cindy Soo Yun Tan, Ziyi Yu, Yang Lan, Chris Abell, and Oren A. Scherman. Biomimetic supramolecular polymer networks exhibiting both toughness and self-recovery. *Adv. Mater.*, 29(10):1604951, jan 2017. .
18. Ji Liu, Cindy Soo Yun Tan, Ziyi Yu, Nan Li, Chris Abell, and Oren A. Scherman. Tough supramolecular polymer networks with extreme stretchability and fast room-temperature self-healing. *Adv. Mater.*, page 1605325, mar 2017. .
19. S. Rose, A. Prevoteau, P. Elzière, D. Hourdet, A. Marcellan, and L. Leibler. Nanoparticle solutions as adhesives for gels and biological tissues. *Nature*, 505:382–385, 2014.
20. E. A. Appel, X. J. Loh, S. T. Jones, C. A. Dreiss, and O. A. Scherman. Sustained release of proteins from high water content supramolecular polymer hydrogels. *Biomaterials*, 33: 4646–4652, 2012.
21. Y. Lan, X. J. Loh, J. Geng, Z. Walsh, and O. A. Scherman. A supramolecular route towards core-shell polymeric microspheres in water via cucurbit[8]uril complexation. *Chem. Commun.*, 48:8757–8759, 2012.
22. M. J. Rowland, E. A. Appel, R. J. Coulston, and O. A. Scherman. Dynamically crosslinked materials via recognition of amino acids by cucurbit[8]uril. *J. Mater. Chem.*, 1:2904–2910, 2013.
23. M. J. Rowland, M. Atgie, D. Hoogland, and O. A. Scherman. Preparation and supramolecular recognition of multivalent peptide-polysaccharide conjugates by cucurbit[8]uril in hydrogel formation. *Biomacromolecules*, 1:2436–2443, 2015.
24. M. Lewin. *Handbook of fiber chemistry. Boca Raton: CRC Press LLC.* 2007.
25. D. Shah, Porter D., and Vollrath F. Can silk become an effective reinforcing fibre? a property comparison with flax and glass reinforced composites. *Compos. Sci. Technol.*, 101:173–183, 2014.
26. P. Colomban, H.M. Dinh, A. Bunsell, and B. Mauchamp. Origin of the variability of the mechanical properties of silk fibres: 1 - the relationship between disorder, hydration and stress/strain behaviour. *J. Raman Spectrosc.*, 43:425–432, 2012.
27. M. Aslan, G. Chinga-Carrasco, B.F. Sø rensen, and B. Madsen. Strength variability of single flax fibres. *J. Raman Spectrosc.*, 46:6344–6354, 2011.
28. F. Vollrath, D. Porter, and C. Holland. The science of silks. *MRS Bulletin*, 38:73–80, 2013.
29. Z. Shao and F. Vollrath. The effect of solvents on the contraction and mechanical properties of spider silk. *Polymer*, 40:1799–1806, 1999.
30. S. Kelly, A. Sensenig, K.A. Lorentz, and T.A. Blackledge. Damping capacity is evolutionarily conserved in the radial silk of orb-weaving spiders. *Zoology*, 114:233–238, 2011.
31. D. De Tommasi, G. Puglisi, and G. Saccomandi. Damage, self-healing, and hysteresis in spider silks. *Biophys. J.*, 98:1941–1948, 2010.